Three New Eccentric Eclipsing Binary Systems in the OGLE-II Database

Marco Ciocca
Department of Physics and Astronomy, Eastern Kentucky University, 521 Lancaster Avenue, Moore 351, Richmond, KY 40475; marco.ciocca@eku.edu

Stefan Hümmerich
Stiftstr. 4, Braubach, D-56338, Germany; ernham@rz-online.de

Received February 10, 2014; revised April 15, 2014; accepted April 15, 2014

Abstract During a search for new binary stars in the publicly available data from the second phase of the OGLE project (OGLE-II), we have identified three new eclipsing binary systems which exhibit various degrees of eccentricity. We have computed models for all systems using BINARYMAKER3 (BM3) and present model fits, residual plots and basic parameters of the stars, along with detailed information on the BM3 parameters used in the modelling process. Our models—which produce good fits to the observed OGLE-II light curves—provide starting points for further (multicolour photometric and spectroscopic) observations of these interesting binary systems.

1. Introduction

The OGLE I-band database is a searchable database of quality photometric data available to the public. During Phase 2 of the experiment, known as "OGLE-II", I-band observations were made over a period of approximately 1,000 days, resulting in over 10^{10} measurements of more than 40 million stars. This was accomplished by using a filter with a passband near the standard Cousins I_c.

Extended searches for previously unrecorded eclipsing binary systems in the OGLE-II database (Udalski *et al.* 1997; Szymański 2005) have led to the discovery of many previously unrecorded eclipsing binaries (cf. Hümmerich and Bernhard 2012; Ciocca 2013). In the present paper, we present details for three eclipsing binary stars exhibiting various degrees of eccentricity. We have computed preliminary models for all systems using BINARYMAKER3 (Bradstreet and Steelman 2004; hereafter BM3). Because OGLE-II photometry is limited to one passband (near Cousins I_c), these models of necessity include a number of assumptions and are limited in the range of information they provide. However, they still reveal a plethora of information and might serve as starting points for further investigations of these interesting systems.

2. Essential data

We have derived magnitude ranges, periods, and epochs of the present objects from an analysis of OGLE-II I-band data. Calculation of periods and epochs were done using PERIOD04 (Lenz and Breger 2005) and PERANSO (Vanmunster 2011). An overview providing essential data of all systems studied in this paper is given in Table 1.

3. Notes on individual objects

3.1. OGLEII CAR-SC3 83135

The OGLE-II database provides 410 observations for this object collected over a time span of 1,265 days. Light curve and phase plot of OGLEII CAR-SC3 83135 (period P = 1.599808 days and eccentricity e = 0.02) are shown in Figure 1.

A visual inspection of the light curve suggests a slight displacement of the secondary minimum from phase $\phi = 0.5$, which becomes more evident when zooming on the corresponding part of the phase plot (compare Figure 2). The secondary minimum actually occurs at phase $\phi = 0.52$, which is indicative of a slightly elliptical orbit. Furthermore, the observed rise in magnitude between phases $\sim 0.1 < \phi < \sim 0.4$ and the corresponding decline between phases $\sim 0.6 < \phi < \sim 0.9$ is indicative of reflection effect (compare, for example, Ruciński 1969; Vaz 1985).

The occurrence of a significant reflection effect in the light curve indicates the presence of a hot (and young?) star. This assumption is also strengthened by the slight eccentricity of the orbit and the relatively short orbital period; an aged system should—under normal circumstances—likely be showing a near-perfect circular orbit.

Additionally, the system is situated well inside the boundaries of a galactic HII region (G291.1-00.8; #999 of Paladini *et al.* 2003) which—according to the aforementioned authors—is centered on the coordinates R.A. $11^h\ 10^m\ 14.8^s$ Dec. –61° 19' 30" (J2000) and has an angular diameter of 4.4 arc minutes. Thus, OGLEII CAR-SC3 83135 is situated only about 47 arc seconds from the center of G291.1-00.8. An inspection of the corresponding sky region on ESO R-plates using ALADIN (Bonnarel *et al.* 2000) shows that the variable is actually embedded in nebulosity (see Figure 3), although it is impossible to tell if the star is associated with the HII region or a foreground object.

On grounds of the above-mentioned suppositions, we have chosen to base our model on the assumption of the presence of at least one young and hot star which is well inside its Roche lobe. From our computed model, which produces a very good fit to the observed light curve, we derive a mass ratio near 0.5 (according to BM3 convention, the mass ratio is always reported as the less massive star over the more massive one, thus resulting in less than unity),

Table 1. Essential data on the eclipsing binaries studied in this paper, sorted by right ascension.

Identifiers	*R.A. (J2000)* *h m s*	*Dec. (J2000)* *° ′ ″*	*Type*	*Range (I_c)*	*Period (d)*	*Epoch (HJD)*	*J–K*[3]
OGLEII CAR-SC3 83135[2] USNO-B1.0 0286-0280163 2MASS J11101357-6120172	11 10 13.570	–61 20 17.27	EA	16.29–16.55	1.599808	2451264.680	0.932
OGLEII CEN-SC1 63647[2] USNO-B1.0 0270-0493821 2MASS J13574324-6255346 UCAC4 136-105327	13 57 43.249	–62 55 34.70	EA	14.40–14.64	3.609794	2451288.65	0.388
OGLEII SCO-SC3 44645[2] USNO-B1.0 0454-0511525 2MASS J16425583-4435497	16 42 55.835	–44 35 49.79	EA	15.35–15.80:	2.736872	2451256.781	0.797

Notes: 1. Positional data from UCAC4 (Zacharias et al. *2012); 2. Positional data from 2MASS (Skrutskie* et al. *2006); 3. From 2MASS (Skrutskie* et al. *2006).*

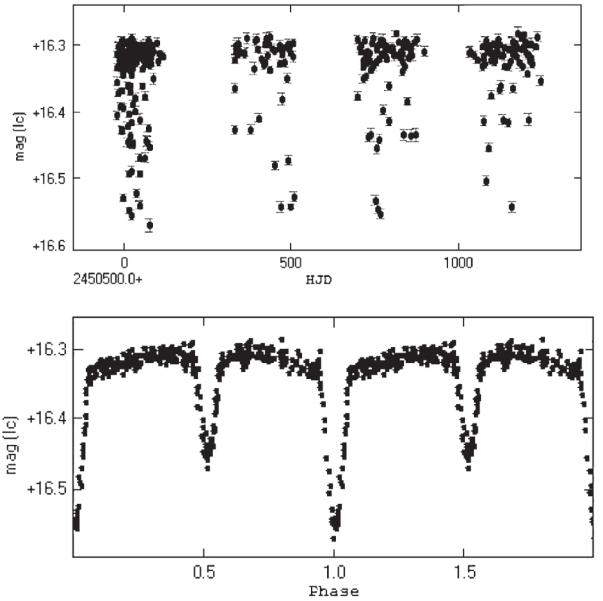

Figure 1. Light curve and phase plot (P = 1.599808 d) of OGLEII CAR-SC3 83135, based on OGLE-II data.

Table 2. BM3-derived parameters for OGLEII CAR-SC3 83135.

Parameter	*Value*
MASS_RATIO	0.5081
FILLOUT_G	–0.322
FILLOUT_S	–0.302
TEMPERATURE_1	11380 K
TEMPERATURE_2	8380 K
GRAVITY_1	1.0
GRAVITY_2	1.0
LIMB_1	0.225
LIMB_2	0.376
REFLECTION_1	1.0
REFLECTION_2	1.0 (1.22, see Figure 4)
THIRD_LIGHT	no evidence
INCLINATION	77.08
SPOTS	no evidence
DISK	no evidence
ECCENTRICITY	0.02

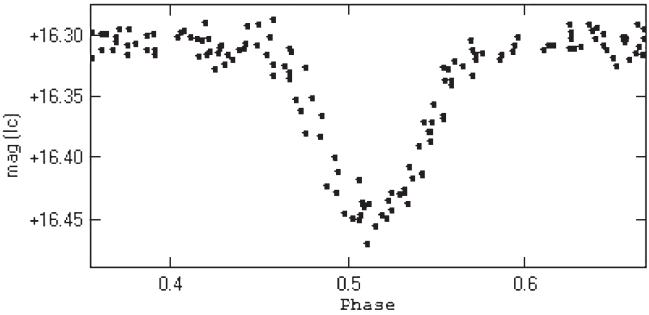

Figure 2. Phase plot of OGLEII CAR-SC3 83135 (detail), illustrating the slight displacement of the secondary minimum which occurs at phase $\phi = 0.52$.

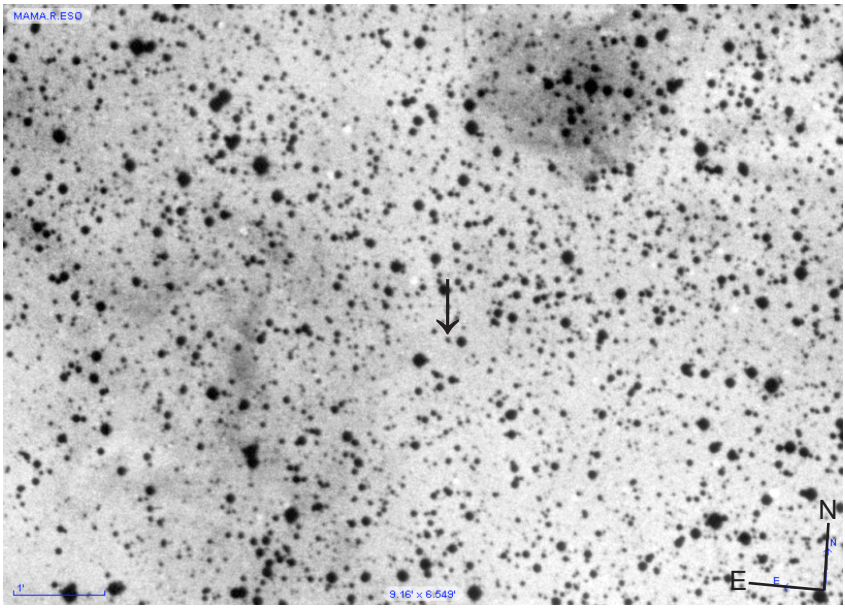

Figure 3. OGLEII CAR-SC3 83135 and its surrounding sky field on an ESO MAMA/CAI R image (accessed via ALADIN). The variable is marked with an arrow. The image is 9.16' × 6.549'. North is up and East is towards the left.

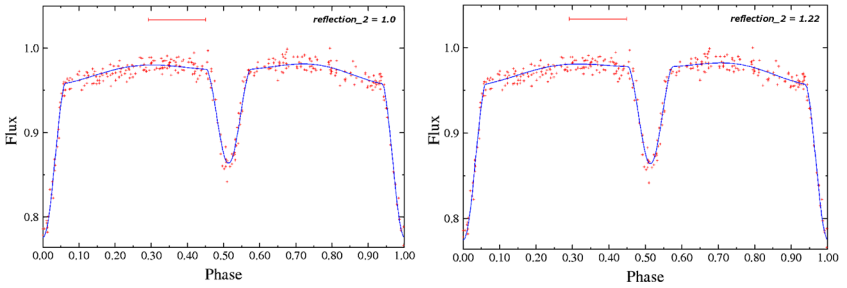

Figure 4. Phase plots of OGLEII CAR-SC3 83135 (crosses) and model fits assuming a value of REFLECTION_2 = 1.0 (solid line, left panel) and REFLECTION_2 = 1.22 (solid line, right panel). Notice the better fit to the observed light curve between phases ~0.3 < ϕ < ~0.45 (marked in the plot) in the right panel.

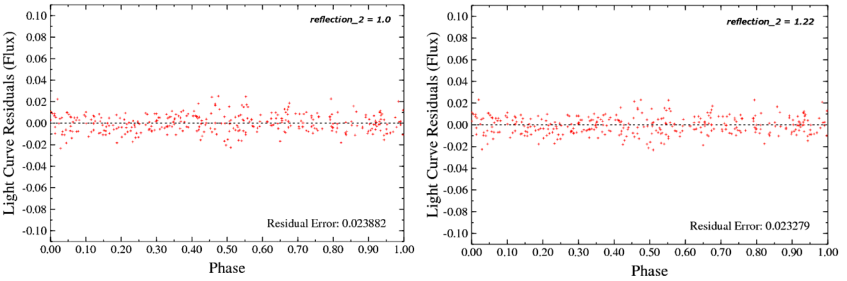

Figure 5. Residual plots of OGLEII CAR-SC3 83135, based on solutions assuming a value of REFLECTION_2 = 1.0 (left panel) and REFLECTION_2 = 1.22 (right panel).

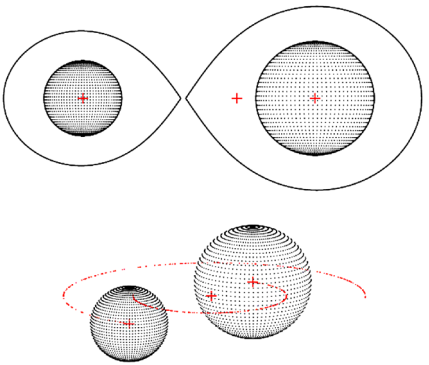

Figure 6. Three-dimensional model and outline of the equipotential surfaces for OGLEII CAR-SC3 83135. The crosses indicate the barycenter of each star and the barycenter of the system, respectively. The circles indicate the orbit of each star.

an inclination of 77.08 degrees, and an eccentricity of only 0.02. Detailed information on the derived BM3 parameters can be found in Table 2.

It is important to note that the best solution was obtained by raising the reflection coefficient REFLECTION_2 to a value of 1.22, which resulted in a noticeably better fit to the observed light curve, in particular between phases ~0.3 < ϕ < ~0.45, and a decrease of the O–C (observed versus computed) error of ~2%. However, a value in excess of 1 is not allowed according to the theory of Ruciński (1969) as a value of 1 already implies that 100% of the flux striking the star is absorbed and re-emitted. This star is embedded in nebulosity, however (see Figure 3), and there could be extra light flux creating this effect. Regardless, as this could not be verified, we have chosen to restrict the corresponding value to 1, which still results in a very good model fit. Figure 4 gives phase plots and model fits for both solutions; the corresponding residual plots are shown in Figure 5. Figure 6 illustrates the corresponding three-dimensional model and the outline of the equipotential surfaces.

We have also computed a solution based on the surmise of a hot spot which also produces a reasonable though slightly inferior fit. However, at this point, we do not see evidence for spot activity in the light curve. Above that, it has to be kept in mind that—because of the data source consisting of information in only one passband—it is to be expected that there will be alternative models producing reasonable accordance with the observed light curves, which also holds true for the other stars presented in this paper.

A brief explanation of the parameters used in these models is necessary (for a far more detailed account see Bradstreet 2005). As mentioned previously, mass ratio q is defined as $Q = M_2/M_1$ where—according to BM3 convention —M_2 is the mass of the less massive and cooler star. The fillout parameter indicates how much of the inner Lagrangian surface of a star is filled by the gas envelope. Negative values indicate that the star does not fill the inner Lagrangian surfaces and correspond to detached systems; positive values indicate (over)contact. Temperature values describe the surface temperatures of the system's components.

Gravity brightening coefficients are used to indicate whether a star is in convective or radiative regime. For a derived surface temperature of $T \leq 7200$ K, stars are treated as convective and a gravity brightening coefficient of 0.32 is assumed. Higher surface temperatures are mostly indicative of radiative stars, in which case a coefficient of 1.00 is standard. Limb darkening parameters are used to evaluate the fading of the surface brightness towards the edges or limbs of the stars. These values are wavelength dependent and are tabulated in the BM3 manual. The reflection parameters have already been discussed above; for radiative stars ($T > 7200$ K), these parameters are usually equal to 1.

3.2. OGLEII CEN-SC1 63647

Due to differences in coverage of the various OGLE-II fields, there are only

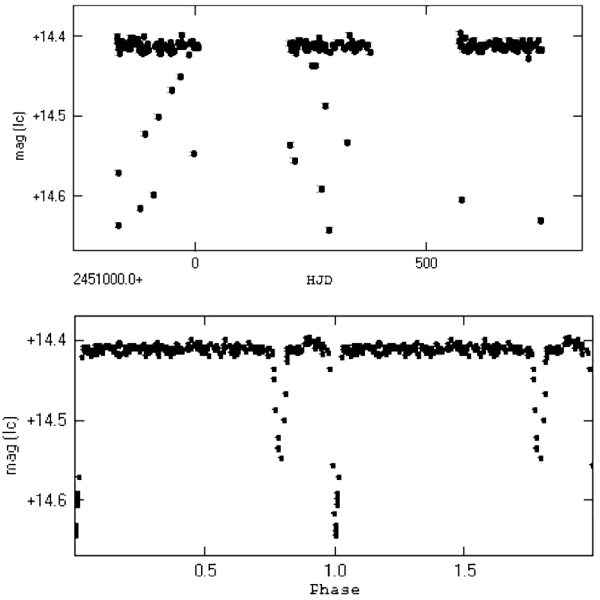

Figure 7. Light curve and phase plot (P = 3.609794 d) of OGLEII CEN-SC1 63647, based on OGLE-II data.

235 observations for this object which were collected over a time span of 915 days. Light curve and phase plot of OGLEII CEN-SC1 63647 (P = 3.609794 days and e = 0.45735) are shown in Figure 7.

Even from a casual inspection of the light curve, the pronounced eccentricity of this system is readily visible, with the secondary minimum occurring at phase $\phi = 0.79$. Additionally, there is a noticeable "hump" between secondary and primary minimum ($\sim 0.83 < \phi < \sim 0.96$). This is obviously due to the tidal distortion of the stars near periastron, when the observer from Earth sees a larger surface (as, for example, in W Ursae Majoris-type variables) and therefore a brighter object. The stars will only be of ellipsoidal shape when near periastron, as in their eccentric orbit they will otherwise be too far apart to be influenced by each other and just be spherical. The amplitude of this effect amounts to ~0.15 mag (I_c), which puts additional constraints on modelling attempts.

We have based our model on the assumption of two hot and young stars because a configuration like this (high eccentricity, relatively short orbital period) would be difficult to explain otherwise. Assuming stars well within their Roche lobes, we were able to compute a model for OGLEII CEN-SC1 63647 which produces a solid fit to the observed light curve. From this, we derive a mass ratio of 0.761, an inclination of 82.1 degrees, and the very high eccentricity of 0.45735. However, further uncertainties—especially concerning the exact shape of the minima—are introduced due to the sparse data for this

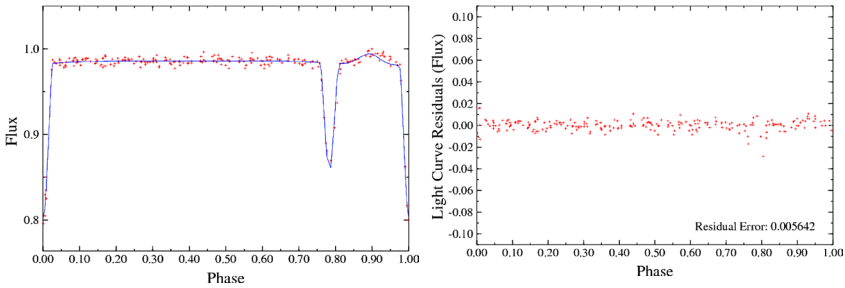

Figure 8. Left panel shows phase plot of OGLEII CEN-SC1 63647 (crosses) and model fit (solid line). Right panel shows the corresponding light curve residuals.

Table 3. BM3-derived parameters for OGLEII CEN-SC1 63647.

Parameter	*Value*
MASS_RATIO	0.761
FILLOUT_G	-0.321
FILLOUT_S	-0.437
TEMPERATURE_1	13485 K
TEMPERATURE_2	11080 K
GRAVITY_1	1.0
GRAVITY_2	1.0
LIMB_1	0.3
LIMB_2	0.23
REFLECTION_1	1
REFLECTION_2	1
THIRD_LIGHT	no evidence
INCLINATION	82.1
SPOTS	no evidence
DISK	no evidence
ECCENTRICITY	0.45735

binary system, to which we attribute the increased scatter seen in the residuals plot around secondary minimum (compare Figure 8, right panel).

Table 3 gives an overview of the BM3 parameters used to produce the present model. Model fit and residual plot are shown in Figure 8. Figure 9 illustrates the corresponding three-dimensional model and the outline of the equipotential surfaces at apastron and periastron, respectively.

3.3. OGLEII SCO-SC3 44645

This particular system exhibits eccentricity that is in between the two

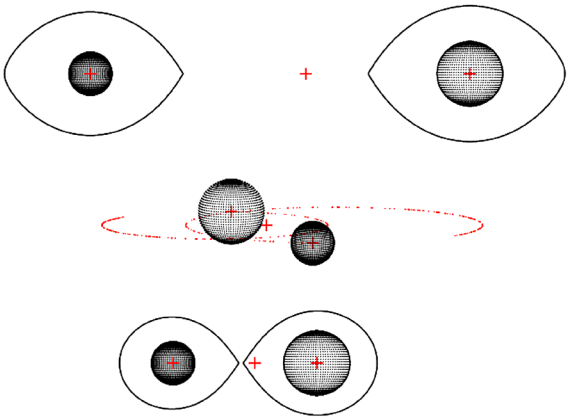

Figure 9. Three-dimensional model and outline of the equipotential surfaces for OGLEII CEN-SC1 63647. The top part shows the equipotential lines at apastron, the bottom part at periastron. The crosses indicate the barycenter of each star and the barycenter of the system, respectively. The circles indicate the orbit of each star.

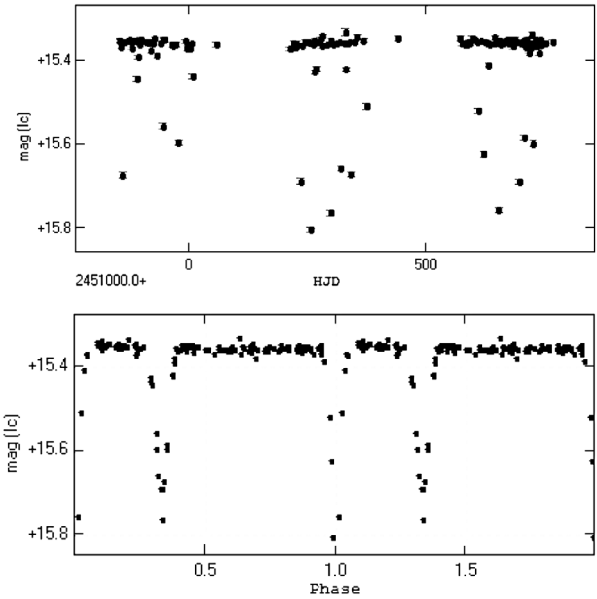

Figure 10. Light curve and phase plot (P = 2.736872 d) of OGLEII SCO-SC3 44645, based on OGLE-II data.

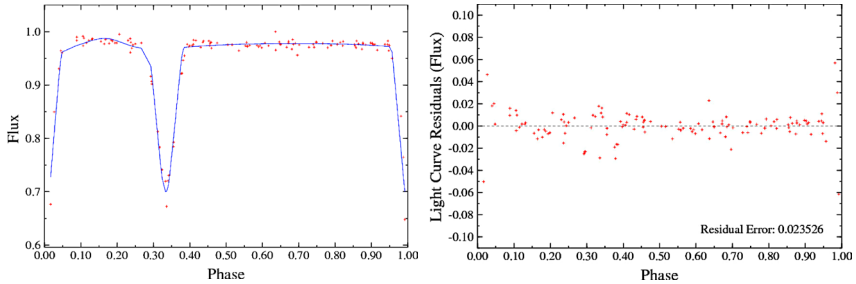

Figure 11. Left panel shows phase plot of OGLEII SCO-SC3 44645 (crosses) and model fit (solid line). Right panel shows the corresponding light curve residuals.

extremes shown before. Unfortunately, it was covered even more scantily; the OGLE-II database comprises only 135 observations taken over the course of 911 days, which adds considerable uncertainty to the derived model solution. Light curve and phase plot of OGLEII SCO-SC3 44645 (P = 2.736872 days and e = 0.2666) are shown in Figure 10; note the weak coverage of minima.

Given the large eccentricity (the secondary minimum occurs at phase $\phi \approx 0.33$), assumptions were made in similar vein to the previous system and the presence of fairly young stars were assumed; with such eccentricity, this system would be hard to conceive otherwise. From our computations, which produce a solid fit to the observations, we derive a mass ratio of 0.601, temperatures of 8115 K and 8305 K for the component stars, an inclination angle of 84.4 degrees, and an eccentricity of 0.2666.

Table 4 gives an overview of the parameters determined in BM3; model fit and residual plot are shown in Figure 11. Figure 12 illustrates the corresponding three-dimensional model and the outline of the equipotential surfaces at apastron and periastron, respectively.

4. Conclusion

We have identified three new eclipsing binary systems in the OGLE-II database which exhibit various degrees of eccentricity. We have computed models for all systems using BINARYMAKER3 which have been based on the assumption of young and hot stars. We present model fits to the observed light curves, residual plots, and basic parameters of the stars which have been derived during the modelling process. Our models—which produce good fits to the observed OGLE-II light curves—provide starting points for further (multicolour photometric and spectroscopic) observations of these interesting binary systems.

Table 4. BM3 derived parameters for OGLEII SCO-SC3 44645.

Parameter	*Value*
MASS_RATIO	0.601
FILLOUT_G	-0.2255
FILLOUT_S	-0.263
TEMPERATURE_1	8115 K
TEMPERATURE_2	8305 K
GRAVITY_1	1.0
GRAVITY_2	1.0
LIMB_1	0.24
LIMB_2	0.38
REFLECTION_1	1.0
REFLECTION_2	1.0
THIRD_LIGHT	no evidence
INCLINATION	84.4
SPOTS	no evidence
DISK	no evidence
ECCENTRICITY	0.2666

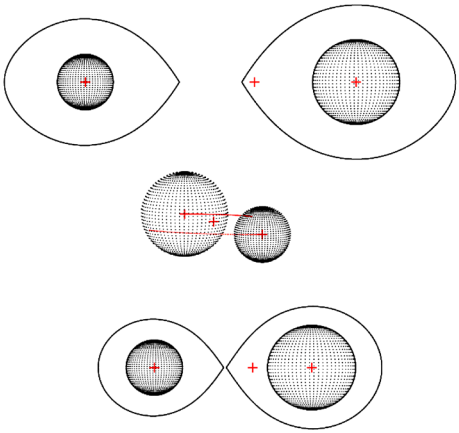

Figure 12. Three-dimensional model and outline of the equipotential surfaces for OGLEII SCO-SC3 44645. The top part shows the equipotential lines at apastron, the bottom part at periastron. The crosses indicate the barycenter of each star and the barycenter of the system, respectively. The circles indicate the orbit of each star.

References

Bonnarel, F. *et al.* 2000, eprint arXiv:astro-ph/0002109.

Bradstreet, D. H. 2005, SASS-24, 23.

Bradstreet, D. H., and Steelman, D. P. 2004, BINARYMAKER3, Contact Software (http://www.binarymaker.com).

Ciocca, M. 2013, *J. Amer. Assoc. Var. Star Obs.*, **41**, 267.

Hümmerich, S., and Bernhard, K. 2012, Perem. Zvezdy, Prilozh., **12**, 11.

Lenz, P., and Breger, M. 2005, *Commun. Asteroseismology*, **146**, 53.

Paladini, R., Burigana, C., Davies, R. D., Maino, D., Bersanelli, M., Cappellini, B., Platania, P., and Smoot, G. 2003, *Astron. Astrophys.*, **397**, 213.

Ruciński, S. M. 1969, *Acta Astron.*, **19**, 245.

Skrutskie, M. F., *et al.* 2006, *Astron. J.*, **131**, 1163.

Szymański, M. K. 2005, *Acta Astron.*, **55**, 43.

Udalski, A., Kubiak, M., and Szymanski, M. 1997, *Acta Astron.*, **47**, 319.

Vanmunster, T. 2011, PERANSO period analysis software (http://www.peranso.com).

Vaz, L. P. R. 1985, *Astrophys. Space Sci.*, **113**, 349.

Zacharias, N., Finch, C., Girard, T., Henden, A., Bartlett, J., Monet, D., and Zacharias, M. 2012, *The Fourth US Naval Observatory CCD Astrograph Catalog* (UCAC4; http://arxiv.org/abs/1212.6182).